DALTON
FULL PAPER

d^{10} Cations within triple-helical cryptand hosts; a structural and modelling study

Michael G. B. Drew,*[a] David Farrell,[b] Grace G. Morgan,[bc] Vickie McKee*[b] and Jane Nelson*[bc]

[a] *Department of Chemistry, The University, Whiteknights, Reading, UK RG6 2AD*
[b] *Schoool of Chemistry, Queens University, Belfast, UK BT9 5AG*
[c] *Chemistry Department, Open University, Milton Keynes, UK MK7 6AA*

Received 22nd December 1999, Accepted 8th March 2000
Published on the Web 10th April 2000

Dicopper(I) analogues of disilver(I) iminocryptates show intercationic separations substantially larger, by as much as 1.5 Å, than do their disilver(I) analogues. This has been confirmed *via* X-ray crystallography of the tris(ethylene)-capped cryptate $[Cu_2L^3][BPh_4]_2$, **1**, and the tris(trimethylene)-capped cryptate $[Cu_2L^2][ClO_4]_2$, **2**, for comparison with structurally characterised disilver analogues. A heterobinuclear Ag^I–Cu^I cryptate $[CuAgL^2][ClO_4]_2$, **3**, with an intermediate M · · · M′ internuclear distance has also been synthesized. These cryptates have been studied by solution ^{1}H NMR and solid state MAS CP ^{13}C and ^{15}N spectroscopy, and compared with the disilver analogues of these and related cryptand hosts. Although both copper(I) and silver(I) cations are formally closed shell systems, density functional calculations show non-zero bond order between the silver cations. The ^{1}H NMR solution spectra reveal the presence of only one conformer for all dicopper cryptates studied, as well as for the tris(ethylene)-capped disilver analogues, while in the tris(trimethylene)-capped disilver systems several conformers coexist in solution.

The well demonstrated tendency of silver(I) cations to aggregate, despite the formal d^{10} character which would appear to rule out bonding interactions, has for some years been a source of puzzlement to co-ordination chemists working in the field of silver complexes as well as one of increasing interest to theoreticians.[1,2] We have encountered the phenomenon in the course of synthesis of azacryptate systems,[3,4] for which Ag^+ is a reliable template ion, eqn. (1).

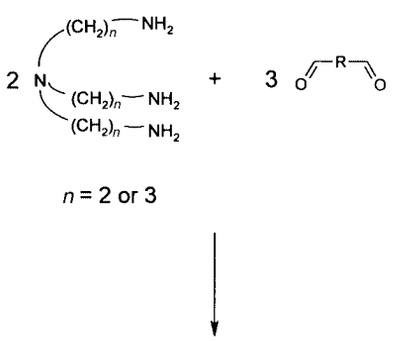

(1)

In the metal(I) templated [2 + 3] Schiff-base condensation reaction between triamines and dialdehydes, $R(CHO)_2$, we have noticed that where R presents little steric hindrance, *e.g.* where the chosen aldehyde is 2,5-diformylfuran,[4–6] disilver cryptates adopt conformations which allow relatively close approach of the encapsulated metal cations. At first sight surprisingly, this close approach is not observed with dicopper(I) analogues[5] such as Cu_2L^1, where Cu^+–Cu^+ internuclear separations are substantially longer than the analogous Ag^+–Ag^+ distances. The cryptand hosts accommodate such differences in co-ordination site separation preference by various low-energy mechanisms for adjusting internuclear separation including, for example, operation of a triple-helical twist. We wish to discover the extent to which the contraction of M · · · M distance in the disilver cryptates results from electronic factors such as intercationic attractive interactions. In this work, therefore, we describe the results of ADF modelling calculations carried out on a pair of d^{10}/d^{10} systems: homobinuclear disilver(I) and dicopper(I) aggregates encapsulated within the furan-spaced, tris-ethylene (tren) capped cryptand L^1 and compare them with structural data obtained for this system and its tris-trimethylene (trpn) capped analogue L^2. Complexes of the related *m*-xylyl spaced cryptands L^3 and L^4 are also discussed.

Results and discussion

In order to compare dimensions in the various dicopper and disilver cryptates, we have examined the more flexible cryptand hosts, avoiding those with *p*-xylyl or thiophene spacers where, because of the dominant steric demands of the host, the disilver and dicopper cryptates are isomorphous[3] or nearly so. The *m*-xylyl spaced hosts L^3 and L^4 are an intermediate case;[4,7] here steric hindrance prevents the closest approach of cations in the disilver cryptates, but substitution of dicopper for disilver still results in sizeable extension of the intercationic separation. In the L^1–L^4 series we have structurally characterised[5] the cryptate $[Cu_2L^1]^{2+}$ as has Martells group[8] the cryptate $[Cu_2L^4]^{2+}$, but $[Cu_2L^2]^{2+}$ and $[Cu_2L^3]^{2+}$ have not so far been subject to X-ray crystallographic study. To complete the comparison matrix, we needed to prepare both these complexes in a form suitable for crystallography.

The complex $[Cu_2L^3]^{2+}$ was readily synthesized by treatment of the "free" ligand (synthesized by [2 + 3] Schiff-base condensation[7]) with Cu^I, and isolated as the BPh_4^- salt, **1**. This was recrystallised from MeCN–EtOH to give X-ray quality crystals. The complex $[Cu_2L^2]^{2+}$ can be prepared *via* the copper(I) template approach, using tris(aminopropyl)amine in an acetonitrile–alcohol solvent mixture and isolated as the ClO_4^- salt, **2**. In early attempts to synthesize this cryptate we carried out a transmetallation reaction using the disilver analogue as starting material. Perhaps unsurprisingly, given the short Ag · · · Ag

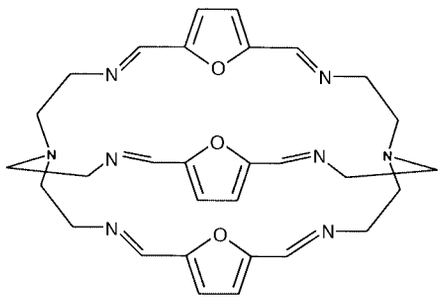

L^1

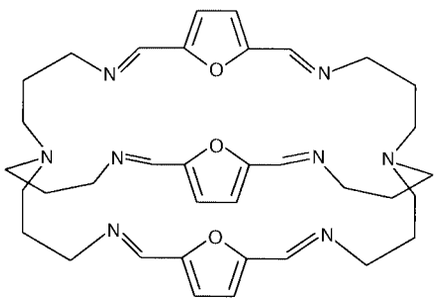

L^2

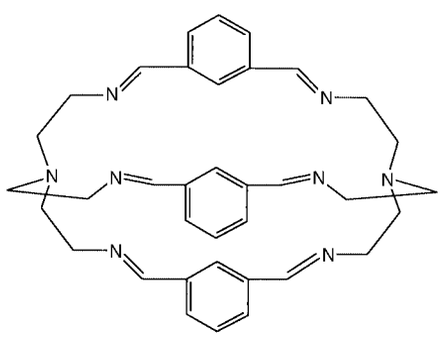

L^3

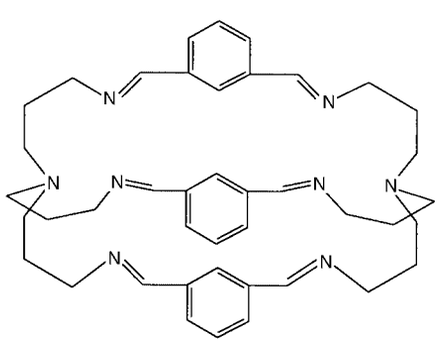

L^4

separation in the starting material,[4] this reaction proved more difficult than we had expected on the basis of earlier experience of transmetallations of disilver macrocyclic complexes.[9,10] Forcing conditions (large excess of Cu^I together with prolonged reflux) were necessary to enable formation of the dicopper(I) product, **2**, and this was normally found as a minor constituent of the reaction mixture together with other products including the unchanged disilver cryptate. Where milder conditions were used, very little if any dicopper(I) product was obtained, and the main transmetallation product was the heterobinuclear Cu^IAg^I cryptate, **3**.

Examination of the ^{1}H NMR spectra (Table 1) of the dicopper(I) cryptates **1** and **2** confirmed that, as in most other dicopper(I) cryptates,[3–5,11–14] the conformations are already frozen at 298 K so that each methylene-cap signal is differentiated into axial and equatorial resonances. There is evidence for the presence of only one, symmetric, conformation where all three strands and both ends are magnetically equivalent. The CH_{imino} chemical shift of the *m*-xylyl spaced cryptates **1**, **4**, **6** and **7** falls in the range δ 8.29–8.63, around 0.2–0.4 ppm deshielded relative to the furan-spaced analogues **9**, **2**, **5** and **8**. Comparison of the imino-resonance of dicopper(I) *vs.* disilver(I)[4] cryptates of L^2 (Fig. 1) and other hosts shows a ≈0.1–0.2 ppm deshielding co-ordination shift for the disilver(I) relative to the dicopper(I) analogues.

The silver(I)-containing cryptates of the trpn-capped hosts studied so far have all given evidence for the presence of more than one conformer in solution, and the heterobinuclear $[CuAgL^2]^{2+}$ cation, **3**, is no exception as the complex 233 K resonance (Fig. 1) shows. On the basis of the ordered crystal structure reported below only two imino CH resonances are to be expected, whereas even at 298 K, where fluxionality broadens features in the remainder of the spectrum, at least 8 partly overlapped lines are seen in the imino region. Some of the complexity is due to coupling of the imino proton to the spin half isotopes ^{109,107}Ag ($^3J \approx 7$–8 Hz), but the intense δ 8.06 uncoupled signal, together with two weaker singlets on either side, derive from the copper-containing end of the cryptate. The less shielded, doublet-coupled resonances correspond to CH_{imino} from the silver end of the molecule; the 298 K spectrum shows one strong and a pair of overlapped weak doublets. The imino-spectrum thus provides evidence for the existence of at least three distinct conformers of the heterobinuclear cryptate in solution at or below ambient temperature. (The evidence from the furan resonances at this temperature is less convincing as the pair of broadened singlets observed are still close to coalescence.) At lower temperatures both imino and furano resonances sharpen and become more complex, with increased overlapping, while the spectrum in the methylene region is heavily overlapped and uninterpretable at both temperatures. It is noticeable that the 233 K ^{1}H NMR spectrum of **3** although complex, is sharply resolved and gives no evidence for interchange of cation co-ordination sites in solution on the NMR timescale.

For the dicopper or disilver tren-capped L^3 cryptate **1** or **7** there is no evidence for the existence of more than one conformer in solution. Solid state MAS CP spectra (Table 2) for **1** and **1a** indicate that the solution conformation is very similar to that observed in the solid state. For these cryptates, in the ^{13}C NMR MAS spectrum, a relatively broad C_{imino} signal close to δ 165 and a pair of methylene cap signals around δ 60–62 and 58–59 confirm the relatively high symmetry of this cryptate in the solid state; the corresponding resonances in the CD_3CN solution spectrum of **1** and **1a** appear at δ 164.8, 61.7 and 57.6. The aromatic region δ 117–137 of **1** is complicated by the presence of overlapping BPh_4^- resonances; for **1a** four still partly coupled peaks can be seen in the δ 140–115 region in ^{13}C NMR MAS, those around δ 138, 132 and 117 bearing protons (as shown by the dipolar dephasing experiment) while the substituted carbons are represented by a complex (still partly N-coupled) resonance centred near δ 133. In CD_3CN solutions of **1** and **1a** ^{13}C aromatic resonances appear close to δ 136, 134 and 129, the δ 117 region being obscured by solvent absorption.

Examination of the MAS-CP spectrum of the "free" cryptand L^3 provides no evidence for significant ^{13}C co-ordination shifts, as imino, aromatic and methylene carbon resonances all lie within 5–15 ppm of the position seen for the dicopper and disilver cryptates. The larger changes are noted in the aromatic CH^1 resonance, presumably deriving from the anisotropic shielding effect of the pair of adjacent encapsulated cations; a much more dramatic change in ^{1}H shift for the CH^1 proton (CH^1 designates the aromatic proton adjacent to both imino-substituents) resonance[7] has been noted in CD_3CN solution for

Table 1 ^{1}H NMR spectra[a] of dicopper(I) and disilver(I) cryptates

Cryptate	*T*/K	CH_{imino}	CH_{Ar}	Methylene CHs			Ref.
				α[m]	β[m]	γ[m]	
1 $[Cu_2L^3]^{2+}$[b]	300	8.47 (s)	7.76 (d), 7.69 (t), 9.88 (s)	3.27 (m)	3.15 (d), 2.69 (m)	—	This work[c]
2 $[Cu_2L^2]^{2+}$	298	8.02 (d)[d,e]	6.95 (s)[d]	3.27 (m), ≈1.9[f]	2.65 (t), 1.60 (d)	2.99 (t), 1.85 (d)	This work[c]
3 $[CuAgL^2]^{2+}$	298	8.18,[g] 8.06,[g] 8.00 (w),[g] 8.18 (d),[i,j] 8.16 (d),[i,j] 8.15 (d)[i,j]	7.04 (s), 6.94 (ws) 7.10 (s)[i]	[h]	[h]	[h]	This work[c]
	233	8.12,[g] 8.02,[g] 7.97,[g] 8.17 (dd),[i] 8.15[i,j]–8.11[i–k]	7.03 (s),[g] 7.02 (s),[g] 6.92 (ws),[g] 7.13 (s),[i] 7.12 (s),[i] 7.08 (q)[i]	[h]	[h]	[h]	This work[c]
4 $[Cu_2L^4]^{2+}$	300	8.29 (s)	7.66 (m), 9.61 (s)	3.11 (d), 3.01 (t)	2.33 (m), 1.58 (d)	2.51 (t), 1.84 (d)	4
5 $[Ag_2L^2]^{2+}$	233	8.23 (dd), 8.22–8.18 (m)[k]	7.18 (s), 7.14 (q), 7.10 (s)	[h]	[h]	[h]	4
6 $[Ag_2L^4]^{2+}$[e]	233	8.42 (d)	7.8 (m), 7.73 (m), 9.87 (s)	3.28 (d), 2.57 (t)	1.81 (q), 1.68 (t)	2.99 (t), 1.70 (d)	4
7 $[Ag_2L^3]^{2+}$	233	8.63 (d)	7.84 (d), 7.74 (t), 9.58 (s)	3.51 (t), 3.31 (d)	3.08 (d), 2.65 (t)	—	11
8 $[Ag_2L^1]^{2+}$	233	8.24 (d)	7.17 (s)	3.54 (t), 3.19 (d)	2.96 (d), 2.55 (t)	—	5, 6
9 $[Cu_2L^1]^{2+}$	233	8.16 (s)	7.10 (s)	3.36 (t), 3.15 (d)	3.03 (d), 2.67 (t)		5

[a] Chemical shifts in ppm from TMS, CD_3CN solution; s = singlet, d = doublet, dd = doublet of doublets, t = triplet, q = quartet, m = multiplet, w = weak. [b] BPh_4 peaks not listed. [c] 500 MHz spectrum. [d] Related by NOE experiment. [e] Long range coupling. [f] Obscured by solvent resonance; partly observable at 233 K. [g] Tentatively assigned to Cu-end signal. [h] Complex and uninterpretable spectra. [i] Tentatively assigned to Ag-end signal. [j] $^3J(^{107,109}Ag, ^1H) \approx 7$–8 Hz. [k] Tentative assignments because of overlapping. [l] Major conformer. [m] α, β, γ to the imino-H.

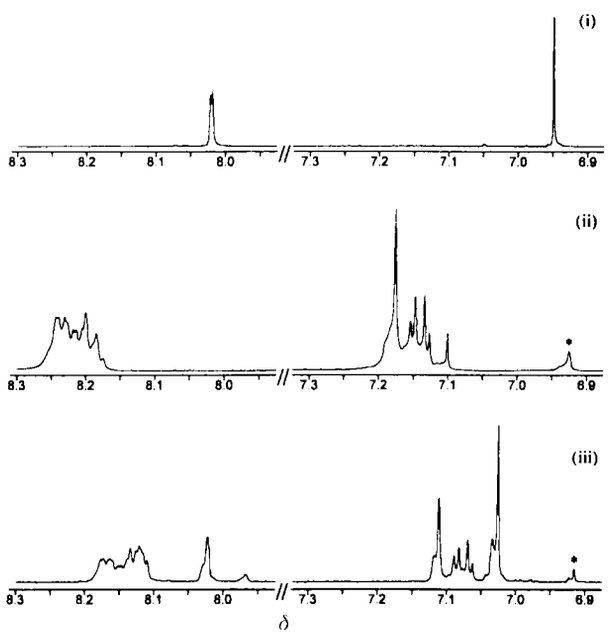

Fig. 1 Comparison of the 233 K ^{1}H NMR spectra of L^2 cryptates in the region δ 8.3–6.9: dicopper(I) **2** (trace (i)); disilver(I) **5** (trace (ii)) and silver–copper **3** (trace (iii)). * = Possible solvent impurity.

these cryptates. Marked co-ordination shifts are however noted in the cryptate ^{15}N imino signals; for **1** and **1a** this resonance appears close to δ −106 *versus* −45 for the "free" cryptand. As noted in MAS CP of other imino complexes of this series;[15,16] there is well defined coupling to ^{63,65}Cu in **1** as shown by the splitting of the imino resonance, although this is not seen for **1a**, which is merely broadened. The disilver L^3 cryptates **7** and **7a** show a much smaller ^{15}N co-ordination shift; the imino resonance is here shifted by only ≈40 ppm, appearing around δ −88 for **7a** and δ −85 for **7**. None of the bridgehead ^{15}N signals of either dicopper or disilver cryptates appear sensitive to encapsulation of the cation, suggesting that this donor is no more than weakly co-ordinating. A weak ^{109}Ag NMR spectrum was obtained for the BF_4^- salt. Unexpectedly this consists of two signals: a weak broad δ ≈588 and a stronger, sharper δ ≈558 resonance. The origin of this splitting is not readily explained as no analogous splitting exists in the ^{13}C or ^{15}N spectra to suggest different co-ordination sites for the silver cations. The possibility for remnant isotopomeric coupling exists, but further studies of MAS spectra of closely spaced silver dimers would be needed before such an explanation could be seriously considered.

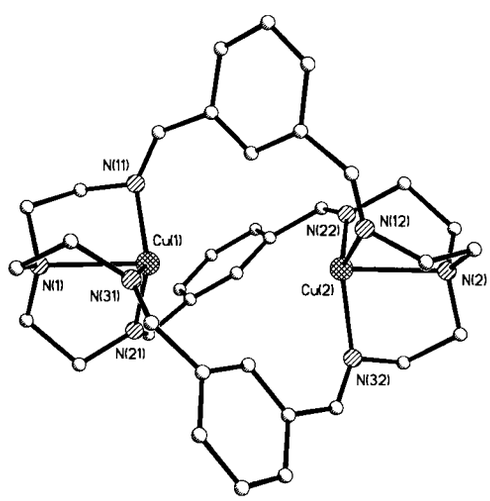

Fig. 2 Structure of $[Cu_2L^3][BPh_4]_2$·MeCN, **1**.

X-Ray crystallography

The crystal structure of complex **1** (Fig. 2) shows a M···M internuclear separation, at 4.23 Å, longer by *ca.* 0.8 Å than in the disilver analogue **7a′**.[4] There is a significant deviation from planarity in the bis-iminophenylene moiety, something that has also been noted[3,8] in the trimethylene-capped dicopper(I) analogue, **4**, and may derive from steric crowding in the central region of the crypt. Torsion angles N=C(CCC)C=N, in **1** and **4** are 36.2 and 45.5° respectively; in the disilver analogues[4,6] **6** and **7a′** these angles are lower at 25.2 and 15.4° respectively, so more severe steric crowding appears to be associated with co-ordination of the smaller cation. In the trpn-capped cryptate[4] $[Ag_2L^4]^{2+}$ **6** we note an M···M contraction of around 0.7 Å compared with the dicopper case[8] **4** which suffers a small but significant (≈0.21 Å) extension of the intercationic separation compared with the tren-capped dicopper analogue, **1** (Table 3). The M–H(C_{ar}) distances in these *m*-xylyl spaced cryptands are all fairly short, on the verge of what might be considered agostic bonding; however as these short contacts are present in both disilver and dicopper systems they may derive from steric necessity rather than choice.

Table 2 MAS-CP spectra of L^3 cryptates

Compound	Spectrum	N_{br}	imino-signal	Ar^2	Ar^4	Ar^3	Ar^1	Methylene
L^3 [a]	^{13}C [b]	—	160	138	133.9	128.4 (m)	126.6 [c]	61.6; 59.9; 57.4 [d]
	^{15}N [e]	−345.5	−45; −41 to −37 (m) [d]					
1a $[Cu_2L^3][BF_4]_2$ [f]	^{13}C	—	167 (m)	134–132	136	139	117.3	62.2; 58.9
	^{15}N	−354.1	−105.9					
7a $[Ag_2L^3][BF_4]_2 \cdot 2H_2O$	^{13}C	—	168.5	130–135 (m)	132.5 ol	139.4	113.1	61.0
	^{15}N	−351 (w), (m) [d]	−88 (w br) [d]					
1 $[Cu_2L^3][BPh_4]_2 \cdot MeCN$ [g]	^{13}C		163.4 (br)	136–132 (m)	ol	137.8 [c]	117.4 [c]	60.4; 58.6 (br)
	^{15}N	−355.9	−93 −(−117) (m) [d]					
7 $[Ag_2L^3][CF_3SO_3]_2$	^{13}C	—	168.7, 166.5	132–135 (m)	136.6	140.3	113.1	62.3, 59.8
	^{15}N	−353.1, −351.5	−84.8, −92.7 (m) [d]					

[a] ^{13}C CD_3CN solution spectrum, ppm from TMS: imino-C 160; Ar C 136.2, 131.5, 128.6, 126.0; methylene C 59.4, 55.0. [b] In ppm from TMS. [c] Tentative assignment due to overlapping. [d] Noisy spectrum, splitting uncertain. [e] In ppm from NH_4 N*O_3. [f] ^{13}C CD_3CN solution spectrum, ppm from TMS: 164.8, 136.4, 133.6, 129.4, 117.5, 61.7, 57.6. [g] ^{13}C CD_3CN solution spectrum, ppm from TMS (BPh_4 peaks omitted): 164.8; 136.4, 133.6, 129.4; 61.7, 57.6. ol = Overlapped.

Table 3 Selected dimensions of cryptates [a]

Cryptate	M ··· M/Å	$M–N_{imino}$ [a]/Å	$M–N_{br}$ [a]/Å	M–O_{fur} or M–H_{ar} [a]/Å	N=CRC=N torsion [b]/°	Dihedral $C–N_{br}M–N_m$ [b]/°	Dihedral $C–N_{br}\cdots N_{br}–C$ [b]/°	$N_{im}–M–M–N_{im}$ torsion/°	Ref.
1 $[Cu_2L^3]^{2+}$	4.23	1.99	2.33	2.67	36.2	5.4	99.1	88.2	This work
2 $[Cu_2L^2]^{2+}$	4.536	2.014	2.25	3.095	45.0	38.6	−172.3	109.4	This work
3 $[CuAgL^2]^{2+}$	3.67	2.047, [c] 2.26 [d]	2.28 [c], 2.51 [d]	3.01, [c] 2.85 [d]	−32.7	−19.0, [d] −46.2 [c]	−173.1	−107.9	This work
4 $[Cu_2L^4]^{2+}$	4.44	2.09	2.28	2.67	−45.5	−42.7	167.3	−107.3	7
5 $[Ag_2L^2]^{2+}$	3.048	2.338	2.506	2.91	16.1	17.6	140.0	104.8	4
6 $[Ag_2L^4]^{2+}$	3.775	2.324	2.42	2.56	−25.2	−11.8, −23.0	−138.3	−103.5	4
7 $[Ag_2L^3]^{2+}$	3.449	2.301	2.553	2.65	15.4	2.5	78.4	73.5	6
8 $[Ag_2L^1]^{2+}$	3.12	2.31	2.69	3.12	−13.8	0.5	77.6	74.1	4
9 $[Cu_2L^1]^{2+}$	4.20	2.00	2.39	3.20	−24.0	−2.1	−83.8	−79.6	5

[a] Average distance and angle, where appropriate. [b] Angles follow the convention defined by Allen and Rogers.[23] [c] M = Copper end. [d] M = Silver end.

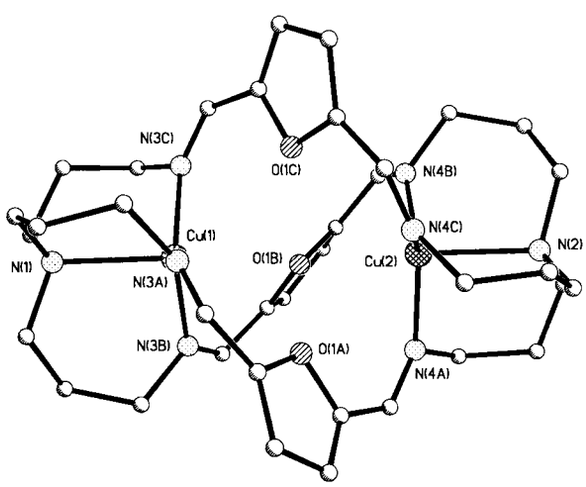

Fig. 3 Structure of $[Cu_2L^2][ClO_4]_2$, **2**.

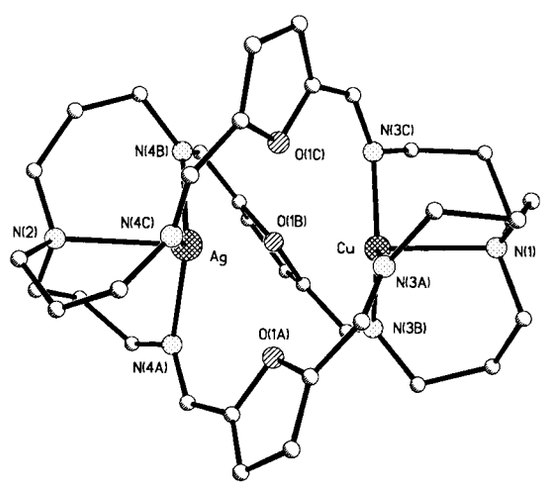

Fig. 4 Structure of $[CuAgL^2][ClO_4]_2$, **3**.

In the furano-spaced system the internuclear M ··· M distance in $[Cu_2L^2]^{2+}$ **2** (Fig. 3) is almost 1.5 Å longer, at 4.54 Å, than in its disilver(I) analogue[4] **5**, a substantially larger difference than the 1.08 Å apparent between the tren capped L^1 pair, **8** and **9**,[5,8] suggesting that the less constrained nature[4] of the larger cryptand host allows more freedom for operation of the natural preferences of the binuclear assembly. Comparison of the different N=C(COC)C=N torsion angles, at 44.8° (for **2**) as against 16.1° (for **5**), in this pair of structures also indicates some steric crowding in the central region for the dicopper case. In the tren-capped analogues **9** and **8** this torsion angle (average N=C(COC)C=N torsion) difference is smaller but still apparent at 24° (for **9**) *versus* 13.8° (for **8**). In **9** the copper–copper internuclear separation is reduced relative to that in the trpn-capped dicopper cryptate, **2**, by over 0.3 Å. Finally in the heterobinuclear Ag–Cu cryptate **3** (Fig. 4) characterised here the internuclear M ··· M′ separation has a value just less than the mean of the separation in **5** and **2**. In respect of other bond lengths, the M–L distances remain much the same over the series, for the same cation, being as expected around 0.2–0.3 Å larger for Ag^+ than for Cu^+. The $M–O_{furan}$ distances are likewise not much altered across the series, remaining in the range 2.9–3.2 Å.

We tried to correlate the internuclear distance with helicity of the cryptand strands. In order to examine structural parameters which may reflect this property, we evaluated the dihedral angles, $C_\alpha–N_{br}\cdots N_{br}–C_\alpha$ and $C_\alpha–N_{br}–Cu–N_{im}$, together with the $N_{im}–M\cdots M–N_{im}$ angle along a strand, for the series of cryptates (Table 3). It proves surprisingly difficult to establish a correlation between any one parameter and the internuclear

cationic separation. Part of the reason for this is that the geometry of the cation co-ordination sphere varies significantly between silver(I) and copper(I). To take the trimethylene-capped cryptates as an example, the copper(I) ions are held slightly inside the cap while the silver(I) ions are extruded slightly out of it toward each other. This causes differences in the bond angles around the imino C=N donors which affect the intercation separation. Comparing the disilver and dicopper series, the C=N–M angles are closer to the normal 120° in the former, which makes the spacer shorter than where distortions have opened out the angles as seen in the dicopper(I) series. Thus the mechanism for adapting to the preferred internuclear separation of a particular pair of cations is a good deal more sophisticated than operation of a simple helical twist.

Two (not necessarily exclusive) rationalisations for the varying internuclear separations seen in this series suggest themselves. One is mechanical in nature in that the difference in co-ordination site separation may be entirely derived from steric factors operating within the cryptand strands, as modulated by the differing size of the co-ordinated cationic guest. The other explanation is that the close approach of Ag^+ cations is the result of weak electronic interactions between the formally d^{10} cations, described either as arising from polarisability or as correlation energy, in accordance with the theoretical approach taken.[2] Modelling studies were carried out, using an ADF program, to determine the importance of the electronic contribution.

ADF Calculations

These structural features were investigated by Density Functional methods using the ADF program.[17,18] The input model for the calculations was derived from the crystal structure of $[Ag_2L^1]^{2+}$. The model was read into the CERIUS 2[19] software package. Owing to the complexity of the calculation it was decided to impose D_3 symmetry upon the structure. This was done using the above program, although in practice very little change in the structure was required. The level IV triple zeta + polarisation basis set was used for all atoms. Other selected options included unrestricted spin, and the GGA (non-local) method with Becke 88[20] Exchange gradient correction and Perdew 86[21] correlation gradient correction. The cation was given a 2+ charge and no anion was included. Geometry optimisation proceeded in a straightforward fashion after 11 cycles to give an Ag···Ag distance of 3.174 Å compared to a value in the crystal structure of 3.115 Å. The Ag–N(bridgehead) distance was 2.674 Å, the Ag–N(imine) distances were 2.315 Å and the Ag–O distances 3.174 Å, values all within 0.02 Å of those found in the crystal structure.

The calculation was then repeated with copper atoms replacing the silver atoms. Despite the fact that the starting value for the Cu···Cu distance was the converged 3.174 Å, this distance rapidly increased and the structure converged after 17 cycles with a Cu···Cu distance of 4.088 Å which clearly indicates no overlap between the metal atoms. By contrast the metal atom approaches the bridgehead nitrogen atom to give a Cu–N distance of 2.403 Å with Cu–N(imine) and Cu–O distances of 1.941 and 3.080 Å respectively.

Finally, the calculation was repeated with one copper atom and one silver atom. However whatever starting model was chosen, it did not prove possible to converge the SCF.

The two homodinuclear structures are shown in Fig. 5. The predicted M···M distances, which in the ADF model rely on the electronic properties of the metal cation rather than on the geometric and mechanical properties of the cryptate skeleton, reproduce very satisfactorily the observed intercationic and cation–donor distances. They indicate the existence of a small but definite attractive interaction between the disilver(I) but not the dicopper(I) cryptates.

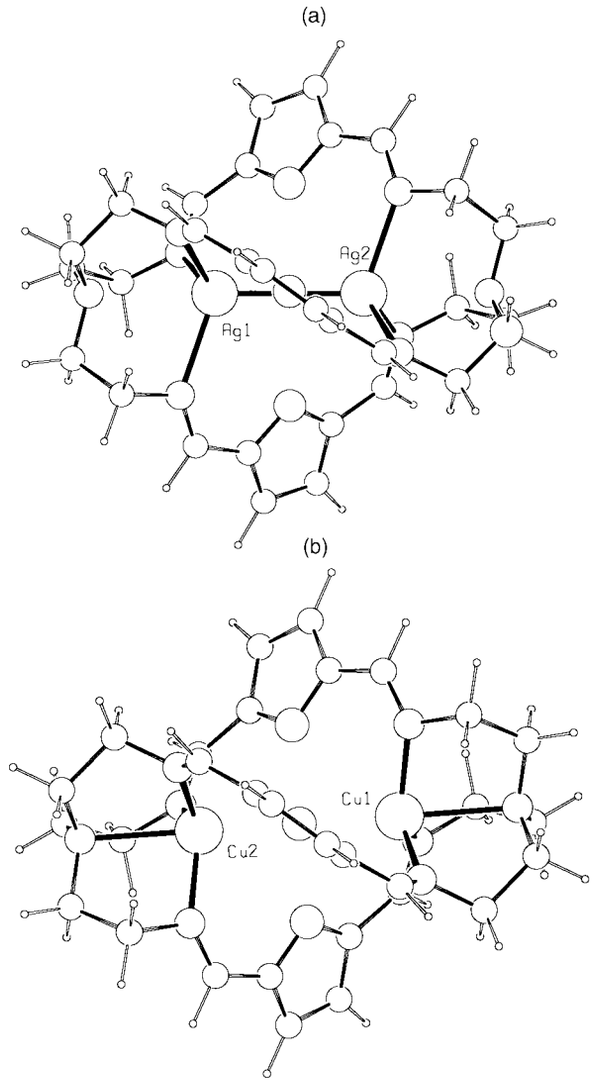

Fig. 5 Structures of complexes **8** (a) and **9** (b) generated by ADF modelling.

On this model the intermediate internuclear distance exhibited by the heterobinuclear Cu···Ag system **3** might be extrapolated to infer approximately half this small electronic interaction. In the trpn-capped disilver analogue **5** the interaction may be expected to be slightly enhanced as the flexibility of the host allows the encapsulated cations more clearly to express their preference for short internuclear separation than in the modelled system, **8**. For the dicopper pair **9** and **2**, the opposite effect is seen, and a slightly larger intercationic distance is the consequence of the increased flexibility of the trpn-capped host. In the case of the *m*-xylyl spaced cryptates **6/7** and **1/4** the intercationic separation is greater with the larger cap in both disilver and dicopper cryptates, in consequence of steric crowding in the central portion of L^4 which generates increased strain on dico-ordination.

In conclusion, it is where a flexible *e.g.* tris-trimethylene cap is used with a sterically undemanding, *e.g.* furano or indeed aliphatic, spacer that we may expect the cryptand host best to accommodate the argentophilic interaction.

Experimental

Syntheses

$[Cu_2L^3][BPh_4]_2\cdot MeCN\cdot H_2O$, 1. To 0.1 mmol of L^3 dissolved in a mixture of 5 cm^3 $CHCl_3$, 20 cm^3 MeCN and 3 cm^3 EtOH was added 0.2 mmol $[Cu(MeCN)_4][ClO_4]$ as a solid, followed by an excess of $NaBPh_4$ as a solid. The amber solution was

Table 4 Crystallographic data for complexes **1**–**3**

	1	**2**	**3**
Empirical formula	$C_{86}H_{85}B_2Cu_2N_9$	$C_{36}H_{49.5}Cl_2Cu_2N_8O_{11.69}$	$C_{39}H_{57}AgCl_2CuN_8O_{12.50}$
Formula weight	1393.33	979.43	1080.24
Crystal system	Monoclinic	Rhombohedral	Monoclinic
Space group	$P2_1/n$	$R\bar{3}$	$P2_1/c$
a/Å	11.033(1)	22.386(4)	15.569(3)
b/Å	47.147(6)	22.386(4)	14.289(4)
c/Å	14.193(1)	45.09(2)	22.001(4)
β/°	95.96(1)		105.75(1)
V/Å^3	7343(1)	19567(10)	4710(2)
Z	4	18	4
μ/mm^{-1}	0.631	1.168	1.048
Reflections collected	10212	5598	7017
independent (R_{int})	9601 (0.0752)	5294 (0.0747)	6141 (0.0643)
Final $R1$, $wR2$ indices [$I > 2\sigma(I)$]	0.0722, 0.1104	0.0814, 0.1756	0.0838, 0.1948
(all data)	0.1722, 0.1444	0.1985, 0.2251	0.1395, 0.2267

allowed to crystallise slowly on standing in air. Amber crystals of X-ray quality were obtained in 81% yield. Found (Calc.): C, 72.5 (72.5); H, 5.9 (6.1); N, 8.5 (8.8)%.

$[Cu_2L^3][BF_4]_2$ 1a. The analogous fluoroborate salt was prepared in around 70% yield by substituting $[Cu(MeCN)_4][BF_4]$ in the above procedure, omitting the addition of $NaBPh_4$.

$[Cu_2L^2][ClO_4]_2$·EtOH 2. To 3 mmol of 2,6-furandialdehyde dissolved in 50 cm^3 degassed MeCN were added 2.7 mmol $[Cu(MeCN)_4][ClO_4]$ in 80 cm^3 degassed MeCN, and finally 0.2 mmol trpn dissolved in 10 cm^3 MeCN under good nitrogen protection and the mixture refluxed for 24 hours. The resulting orange solution was evaporated under nitrogen to around 20 cm^3, 5 cm^3 industrial alcohol were added and the solution placed in an atmosphere of diethyl ether to crystallise. Orange-brown crystals of the dicopper cryptate were obtained in ≈40% yield. Found (Calc.): C, 45.5 (45.1); H, 4.9 (5.4); N, 11.4 (11.1)%.

$[CuAgL^2][ClO_4]_2$ 3. To 0.5 mmol of $[Ag_2L^2][ClO_4]_2$ in 50 cm^3 degassed MeCN were added 1.8 mmol $[Cu(MeCN)_4][ClO_4]$ dissolved in 80 cm^3 MeCN and the mixture refluxed for 3–4 h before reducing to ≈25 cm^3 under nitrogen. To 5 cm^3 of this solution 5 cm^3 of EtOH were added and the mixture left to crystallise in an ether bottle where a mix of orange-red hexagons and pale coloured plates was obtained in ≈30% yield. The red-orange hexagons were picked out for crystallography and for NMR spectroscopy: several selections were made for ^{1}H NMR to minimise the danger of including some of the pale crystals in the selected sample.

$[Ag_2L^3][CF_3SO_3]_2$ 7. Compound L^3 (0.17 mmol) in 5 cm^3 $CHCl_3$ was added to 0.35 mmol of $AgCF_3SO_3$ in a warm solution of 30 cm^3 EtOH–20 cm^3 MeCN. A white microcrystalline product was isolated in 65% yield. FAB-MS: AgL m/z 693, Ag_2L 801 and $Ag_2L(CF_3SO_3)$ 951. Found (Calc.): C, 41.8 (41.5); H, 3.3 (3.7); N, 10.2 (10.2)%. The tetrafluoroborate analogue, $[Ag_2L^3][BF_4]_2$·$2H_2O$ **7a**, was prepared as above in about 80% yield, substituting $AgBF_4$ for $AgCF_3SO_3$. This sample differs from the crystallographically characterised[4] analogue, **7a′**, in respect of solvation. Found (Calc): C, 43.3 (42.7); H, 4.2 (4.5); N, 11.1 (11.1)%.

X-Ray crystallography

All the data sets were collected at 153(2) K on a Siemens P4 diffractometer using Mo-Kα radiation ($\lambda = 0.71073$ Å, $4 < 2\theta < 50°$). Empirical absorption corrections were applied to complexes **2** and **3**. The structures were solved by direct methods and refined by full matrix least squares on F^2, using all the reflections. Full-occupancy non-hydrogen atoms were refined with anisotropic atomic displacement parameters and hydrogen atoms bonded to carbon were inserted at calculated positions with isotropic displacement parameters riding on U_{ij} of their carrier atoms. Hydrogen atoms bonded to oxygen were located for the ethanol solvates in **2** but not for the partial-occupancy water molecules in **3**. Details of the structure determinations are given in Table 4, selected bond lengths and angles in Table 5. All programs used in the structure solution and refinement are contained in the SHELX-97 package.[22]

Table 5 Selected bond lengths [Å] and angles [°] for complexes **1**–**3**

Cu(1)–N(1)	2.342(6)	2.271(10)	2.929(10)
Cu(1)–N(3A)	1.975(6)	2.00(10)	2.041(9)
Cu(1)–N(3B)	1.992(6)	1.987(11)	2.054(10)
Cu(1)–N(3C)	1.969(6)	2.020(12)	2.051(10)
M–N(2)	2.312(6)	2.234(12)	2.509(10)
M–N(4A)	1.996(6)	2.015(11)	2.249(11)
M–N(4B)	1.988(6)	2.030(12)	2.251(10)
M–N(4C)	1.995(7)	2.030(12)	2.264(10)
Cu(1)···M	4.229(1)	4.535(2)	3.674(2)
N(1)–Cu(1)–N(3A)	83.0(2)	92.7(4)	90.1(4)
N(1)–Cu(1)–N(3B)	80.1(2)	94.8(4)	90.9(4)
N(1)–Cu(1)–N(3C)	80.8(2)	94.5(4)	90.3(4)
N(3A)–Cu(1)–N(3B)	112.0(2)	117.9(4)	119.4(4)
N(3A)–Cu(1)–N(3C)	123.1(3)	119.8(4)	120.9(4)
N(3B)–Cu(1)–N(3C)	118.0(2)	120.9(5)	119.7(4)
N(2)–M–N(4A)	81.2(2)	92.8(5)	94.8(3)
N(2)–M–N(4B)	82.6(2)	95.0(5)	85.3(3)
N(2)–M–N(4C)	81.7(2)	93.7(5)	84.0(3)
N(4A)–M–N(4B)	114.2(3)	117.0(5)	118.6(4)
N(4A)–M–N(4C)	117.7(3)	124.1(5)	119.6(4)
N(4B)–M–N(4C)	122.2(3)	117.6(5)	119.3(4)

M = Cu(2) for structures **1** and **2**, Ag for **3**.

CCDC reference number 186/1891.

See http://www.rsc.org/suppdata/dt/a9/a910240j/ for crystallographic files in .cif format.

Acknowledgements

We are grateful to Open University Research Committee and BBSRC for support (to G. G. M. and D. F.). EPSRC are thanked for access to services (FAB-MS at Swansea, solid state NMR at Durham).

References

1 V. W.-W. Yam, K. K.-W. Lo, W. K.-M. Fung and C.-R. Wang, *Coord. Chem. Rev.*, 1998, **171**, 17 and references therein.
2 P. Pyykko, *Chem. Rev.*, 1997, **97**, 597.
3 J. Nelson, G. Morgan and V. McKee, *Prog. Inorg. Chem.*, 1998, **47**, 167.
4 O. W. Howarth, G. G. Morgan, V. McKee and J. Nelson, *J. Chem. Soc.*, *Dalton Trans.*, 1999, 2097.

5 Q. Lu, J.-M. Latour, C. J. Harding, N. Martin, D. J. Marrs, V. McKee and J. Nelson, *J. Chem. Soc.*, *Dalton Trans.*, 1994, 1471.
6 R. Abidi, F. Arnaud-Neu, M. G. B. Drew, S. Lahely, D. Marrs, J. Nelson and M.-J. Schwing-Weil, *J. Chem. Soc.*, *Perkin Trans. 2*, 1996, 2747.
7 C. J. Harding, J. F. Malone, D. J. Marrs, N. Martin, V. McKee and J. Nelson, *J. Chem. Soc.*, *Dalton Trans.*, 1995, 1739.
8 N. P. Ngwenya, J. Ribenspeis and A. E. Martell, *J. Chem. Soc.*, *Chem. Commun.*, 1990, 1207.
9 M. G. B. Drew, B. P. Murphy, J. Nelson and S. M. Nelson, *J. Chem. Soc.*, *Dalton Trans.*, 1987, 873.
10 S. M. Nelson, *Pure Appl Chem.*, 1980, **52**, 2461.
11 C. J. Harding, Q. Lu, D. J. Marrs, G. Morgan, M. G. B. Drew, O. Howarth, V. McKee and J. Nelson, *J. Chem. Soc.*, *Dalton Trans.*, 1996, 3021.
12 M. G. B. Drew, J. Hunter, D. J. Marrs, C. J. Harding and J. Nelson, *J. Chem. Soc.*, *Dalton Trans.*, 1992, 3235.
13 Q. Lu, C. J. Harding, V. McKee and J. Nelson, *Inorg. Chim. Acta*, 1993, **211**, 195.
14 Q. Lu, C. J. Harding, V. McKee and J. Nelson, *J. Chem. Soc.*, *Chem. Commun.*, 1993, 1768.
15 D. Apperley, J. L. Coyle, B. Maubert, V. McKee and J. Nelson, *J. Chem. Soc.*, *Dalton Trans.*, 1999, 229.
16 J. L. Coyle, Ph.D, Open University, 1999.
17 ADF1999, E. J. Baerends, A. Berces, C. Bo, P. M. Boerrigter, L. Cavallo, L. Deng, R. M. Dickson, D. E. Ellis, L. Fan, T. H. Fischer, C. Fonseca Guerra, S. J. A. van Gisbergen, J. A. Groeneveld, O. V. Gritsenko, F. E. Harris, P. van den Hoek, H. Jacobsen, G. van Kessel, F. Kootstra, E. van Lenthe, V. P. Osinga, P. H. T. Philipsen, D. Post, C. C. Pye, W. Ravenek, P. Ros, P. R. T. Schipper, G. Schreckenbach, J. G. Snijders, M. Sola, D. Swerhone, G. te Velde, P. Vernooijs, L. Versluis, O. Visser, E. van Wezenbeek, G. Wiesenekker, S. K. Wolff, T. K. Woo and T. Ziegler, Vrije Universiteit, Theoretical Chemistry, Amsterdam, The Netherlands, 1999.
18 C. Fonseca Guerra, J. G. Snijders, G. te Velde and E. J. Baerends, *Theor. Chim. Acta*, 1998, **99**, 391.
19 CERIUS 2, version 3.5, Molecular Simulations Inc., San Diego, CA, USA, 1998.
20 A. D. Becke, *Phys. Rev. A*, 1988, **38**, 3098.
21 J. P. Perdew and Y. Wang, *Phys. Rev. B*, 1986, **33**, 8800.
22 G. M. Sheldrick, SHELX 97, University of Göttingen, 1997.
23 F. H. Allen and D. Rogers, *Acta Crystallogr.*, *Sect. B*, 1969, **25**, 1326.